

Polyphenol mediating chitin self-assembly for constructing the full natural resourced hydrogel with high strength and toughness

Xinghuan Lin, Lina Zhang and Bo Duan*

¹College of Chemistry and Molecular Sciences, Hubei Engineering Center of Natural Polymer-based Medical Materials, and Key Laboratory of Biomedical Polymers of Ministry of Education, Wuhan University, Wuhan 430072, China

*To whom the correspondence should be addressed: B. Duan (bo_duan@whu.edu.cn)

Methods

Materials. Chitin was provided by Golden-Shell Biochemical Co., Ltd., Zhejiang, China. Tannic acid, gallic acid, pyrogallol, quercetin, protocatechuic acid and porcine pepsin (15000 U/mg) were purchased from Aladdin. Other chemicals were obtained from Sinopharm Chemical Reagent Co., Ltd, Shanghai, China. PBS solution (0.1 M, pH 7.4) was prepared by sodium chloride, potassium chloride, disodium hydrogen phosphate and monopotassium phosphate. Gram-positive *Staphylococcus aureus* (*S. aureus*, ATCC 6538) and Gram-negative *Escherichia coli* (*E. coli*, ATCC 15597) were used in this study.

Preparation of chitin-polyphenol hydrogels. To purify chitin, the raw chitin powder was continuously treated at room temperature with 5 wt% sodium hydroxide (NaOH) for 12 h, 5 wt% hydrochloric acid (HCl) solution for 12 h and 5 wt% NaOH solution for 24 h, and then washed with water after each step. Finally, the treated chitin was treated with 5 wt% hydrogen peroxide for 8 h (pH 9, 80°C), then washed with water and dried at vacuum oven.

4.5 g purified chitin powder was immersed in 30 g 36.7 wt% NaOH aqueous solution at room temperature for 8 h, and subsequently, the suspension was frozen at -40°C in a cooling trap for 4 h and then thawed at 25°C. Then, 70 g distilled water was added into suspension, and the suspension was frozen at -40°C in a cooling trap for 4 h and thawed at 5 °C once~twice times to obtain a 4.31 wt% transparent chitin solution. Besides, 90 g 11 wt% NaOH aqueous solution prepared and 10 g polyphenol powder added to obtain 10 wt% polyphenol solution. A certain amount of 10 wt% polyphenol solution was added into chitin solution to get chitin-polyphenol solution. The chitin-polyphenol solution was placed in 60°C for a certain time to form alkaline

gel. Finally, the alkaline gels were neutralized in different ethanol concentration solution and washed thoroughly with water until the pH of the rinsed water reached to 7.

Characterization. The morphologies of the hydrogels were carried out with an atomic force microscope (AFM, Cypher ES, Asylum Research) in peak force QNM mode. Field emission scanning electron microscopy (FESEM, Zeiss, SIGMA, Germany) was used to characterize morphologies of lyophilized hydrogels, and nanomeasurer software (Department of Chemistry, Fudan University, China) was used to determine the nanofibers diameter and distribution. Fourier transform infrared spectroscopy (FT-IR) of lyophilized hydrogels was tested using a Nicolet 170-SX (Thermo Nicolet Ltd., USA) in the wavenumber range from 4000 to 400 cm^{-1} . The X-ray diffraction (XRD) patterns of the hydrogels were recorded by a Rigaku Smartlab 9000 diffractometer in reflection mode with a scanning speed of $2^\circ \cdot \text{min}^{-1}$ at 200 mA and 45 kV. X-ray photoelectron spectra (XPS, ESCALAB250Xi, Thermo Fisher Scientific, America) analyses were recorded using a Kratos XSAM800 X-ray photoelectron spectrometer. Optical transmittance of the hydrogel with a thickness of 2 mm was observed with a UV-vis spectrometer (UV-6, Shanghai Meipuda Instrument Co.,Ltd., China) at a wavelength from 900 nm to 200 nm. Rheological measurements of the solution were analyzed on a DHR3 rheometer (TA Instruments, Delaware, USA). Raman spectroscopy and spatial Raman mapping were performed using a Raman imaging microscope (Thermo Scientific DXR xi, USA). The wavelength of the excitation laser was 532 nm. A spatial resolution for Raman mappings collected was 200 nm. The collected spectra were preprocessed using cosmic ray removal, noise filtering, and normalization techniques. The MCR method developed by OMNICxi software

was applied for calculating the proportion of interaction domains. Thermogravimetric analysis (TGA) of the lyophilized chitin-tannic acid hydrogels were carried out by a Pyris diamond TA Lab System (PerkinElmer) at a heating rate of 10°C/min from 80°C to 800°C under nitrogen atmosphere.

Swelling ratio and Water content. Swelling ratio and water content of hydrogels were calculated as following equations:

$$\text{Swelling ratio (\%)} = \frac{W_w - W_d}{W_d} \times 100$$

$$\text{Water content (\%)} = \frac{W_w - W_d}{W_w} \times 100$$

where W_w and W_d are the weight of the hydrogel and xerogel (drying at 60°C in vacuum).

Deacetylation degree (DD). DD of chitin was determined by acid base double point potentiometric titration¹. During gelation, the chitin solution and chitin-tannic acid solution were neutralized by 0.1 M HCl solution to obtain precipitates, respectively, and then precipitates were washed thoroughly by water and ethanol and dried at 60°C vacuum oven. m gram of dried powder (about 0.1 g) was dispersed in 20 mL 0.1 M HCl solution and stirred for 12 h. Then, 0.1 mol/L NaOH was titrated, and a titration curve between pH value and corresponding volume of NaOH solution was plotted. This graph had two inflection points, where the corresponding NaOH volumes were recorded as V_1 and V_2 . The DD (%) value was calculated as following equation:

$$DD(\%) = \frac{(V_2 - V_1) \times c \times 0.016}{0.0994 \times m} \times 100$$

Hydrogel disassembly experiments. Hydrogels in 100 mM NaCl, 100 mM urea or 100 mM Tween 20 solution were maintained at 37°C and 100 rpm for the 48 h. Then, hydrogels were utilized for compressive measurements and swelling ratio analysis.

Mechanical property test. Compressive and tensile measurements were tested on the hydrogels using a universal tensile-compressive tester (INSTRON instrument, Model 5576, USA). A columnar hydrogel with a height of about 10 mm and a diameter of 8~12 mm was tested at the speed of 2 mm·min⁻¹. And a hydrogel membrane with a thickness of about 2 mm was measured at the speed of 2 mm·min⁻¹. Cyclic tests were carried out by performing subsequent trials immediately after the initial loading. Young's modulus were calculated from the initial linear region of the stress-strain curves. The fracture energy (toughness) was calculated from full region of the stress-strain curves.

Biocidal efficacy test. *S. aureus* and *E. coli* were used to test the biocidal efficacy of the hydrogels. 20 µL bacterial suspensions (about 4.072×10^7 CFU of *S. aureus* and 4.631×10^7 CFU of *E. coli*, respectively) were added to the center between two pieces of hydrogels (thickness of 2 mm and diameter of 12 mm). After 4 h incubation at 37°C, the hydrogels were vortexed to remove bacteria from hydrogels to PBS solution. 10-fold serial dilutions of the sterilized solutions were prepared with 100 mM PBS solution, and 10 µL of each dilution was transferred onto agar plate, respectively. The agar plates were placed at 37°C for 24 h, and then the bacterial colony counts were calculated for antibacterial properties analysis. The hydrogels after treatment with bacteria were soaked in the PBS solution containing 4 wt%

paraformaldehyde for 2 h at room temperature in order to fix the bacteria onto the hydrogels. A series of graded PBS-alcohol solutions (25%, 50%, 75%, 85%, 90%, 95%, 100% of alcohol) were dehydrated the bacteria. Finally, the treated hydrogels were lyophilized and characterized by SEM.

Toxicity test. According to International Standard Organization (ISO/EN 10993-5), MTT assay was used to investigate the in vitro cytocompatibility of hydrogels with rat skin fibroblasts. The L929 cells were cultured in a medium of Dulbecco's Modified Eagle Medium containing with 10 % fetal bovine serum and 1% penstrip at 37°C under 5% CO₂ atmosphere. An aliquot of 100 µL L929 cells suspension containing about 10⁴ cells was seeded in a 96-well plate. The lyophilized hydrogels were grinded to powder and added PBS solution to prepare 2 mg/mL suspension, at the same time, 2 mg/mL of TA solution was as a control. Then, the suspensions and TA solution were inactivated under UV light for 1 h. After 24 h incubation, the culture mediums were replaced with the inactivated suspensions and solution. After another 24 h incubation, 50 µL of MTT reagent were added to each well and the plate was cultured in dark for 4 h. The absorbance of each well at OD_{490 nm} was measured with a reference wavelength of OD_{690 nm} using a microplate reader (Infinity M200 Pro, Tecan). The pristine L929 cells incubated only in fresh medium were also tested under the same conditions to serve as negative controls.

Simulated gastric fluid (SGF) degradation test. SGF was prepared using ultrapure water at pH value of 1.5 (using by 37% w/v HCl) and then porcine pepsin was added. To ensure porcine

pepsin activity, the SGF is prepared at 37°C approximately 1 h prior to experiments. A concentration of 0.2 mg·mL⁻¹ of pepsin was chosen in this study, because the porcine pepsin concentration ranges from 0.11 to 0.22 mg·mL⁻¹ in the human fasted state². Hydrogels with a length of 5 mm were added in 5 mL PBS, HCl (pH 1.5) and SGF solution, respectively, and all the solutions were incubated at 37°C and with a constant 65 rotations per minute. After a specific time, the hydrogels were taken up and weighed.

Soil degradation test. The hydrogels enclosed respectively in nylon fabrics (500 meshes) were placed in the natural soil under 10 cm deep, and the environment temperature was in the range from 25 to 30°C during test. The degraded samples from the burying time of 0-30 days were examined with a digital photo and SEM and by the mass change from the degradation kinetics. Before weighting, all hydrogels were equilibrated in DI water before testing.

Supplementary Figures

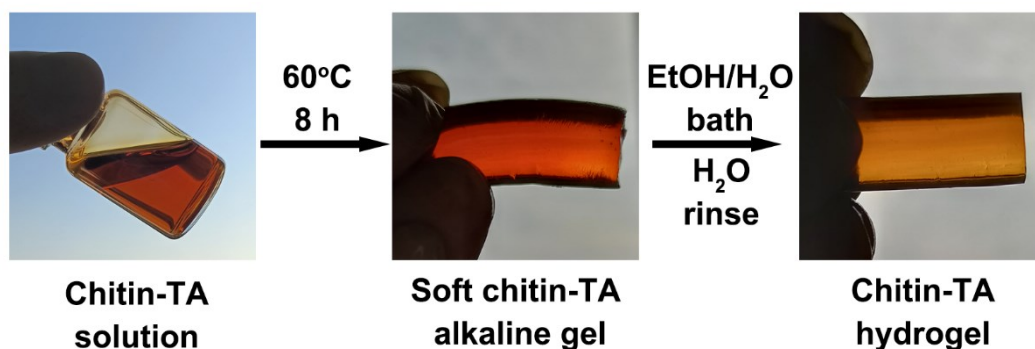


Fig. S1 Preparation of the chitin-polyphenol hydrogel.

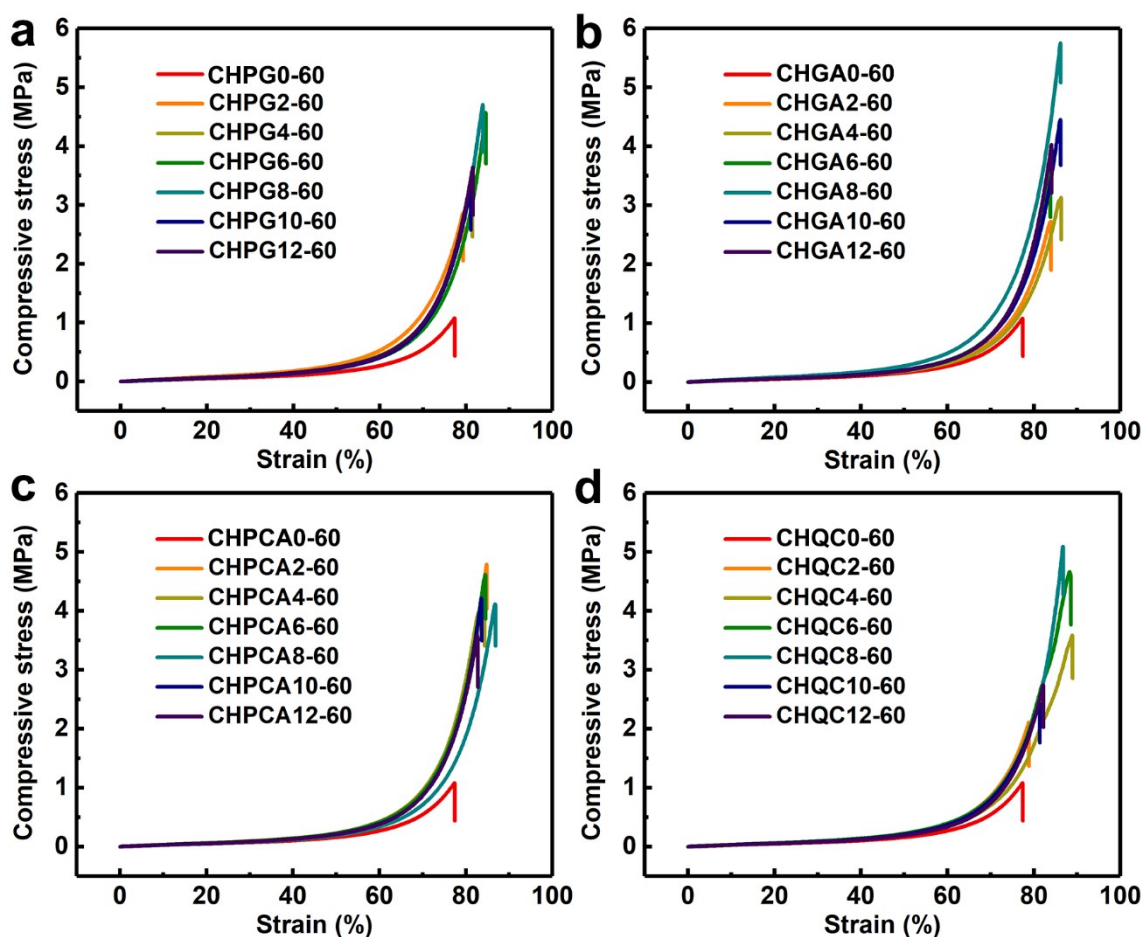


Fig. S2 Compressive stress-strain curves of a) CHPG, b) CHGA, c) CHPCA and d) CHQC hydrogels with different weight ratios of polyphenol to chitin.

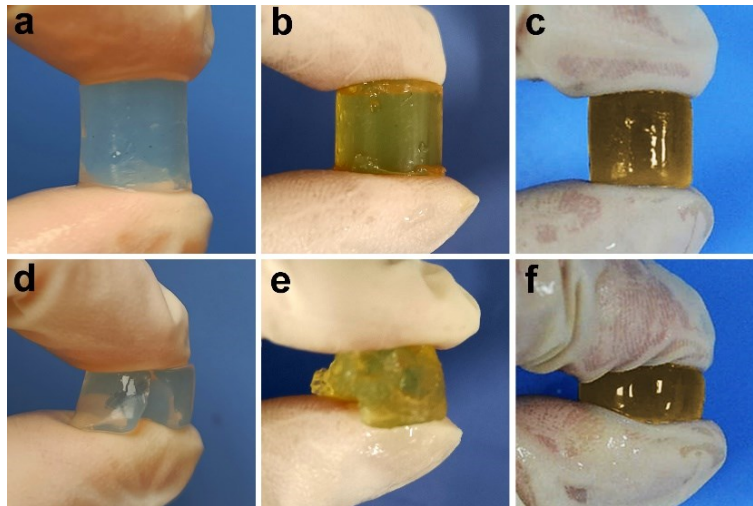


Fig. S3 Photos of compressive behaviours of **a, d)** CHTA0-60 hydrogels, **b, e)** CHTA8 alkaline gels (without ethanol coagulating) and **c, f)** CHTA8-60 hydrogels before and after compression.

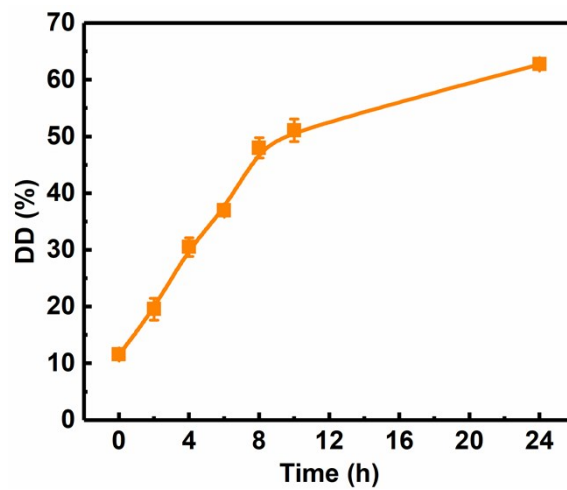


Fig. S4 The deacetylation degree of chitin after heating with different time at 60°C.

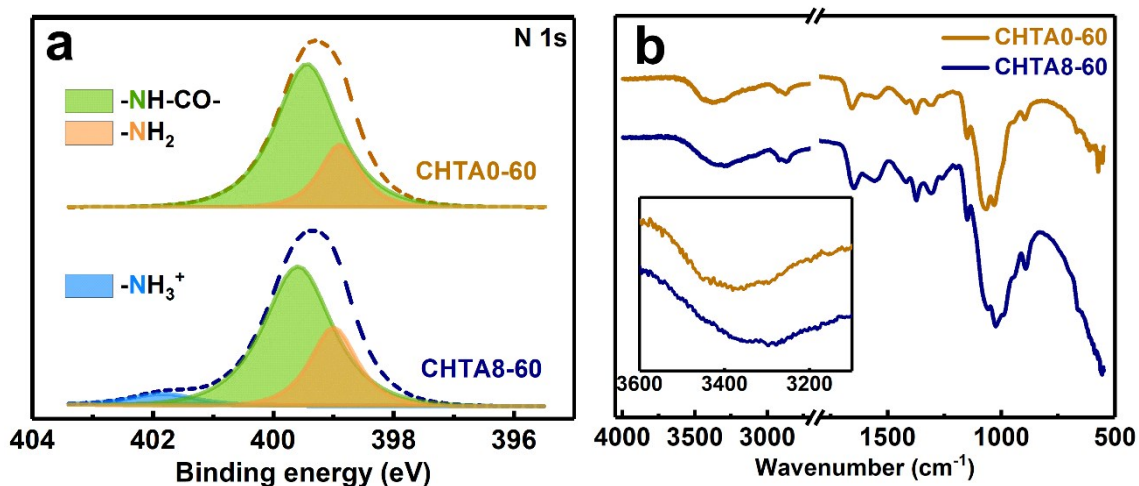


Fig. S5 a) N 1s XPS spectra and b) FT-IR spectra of CHTA0-60 and CHTA8-60.

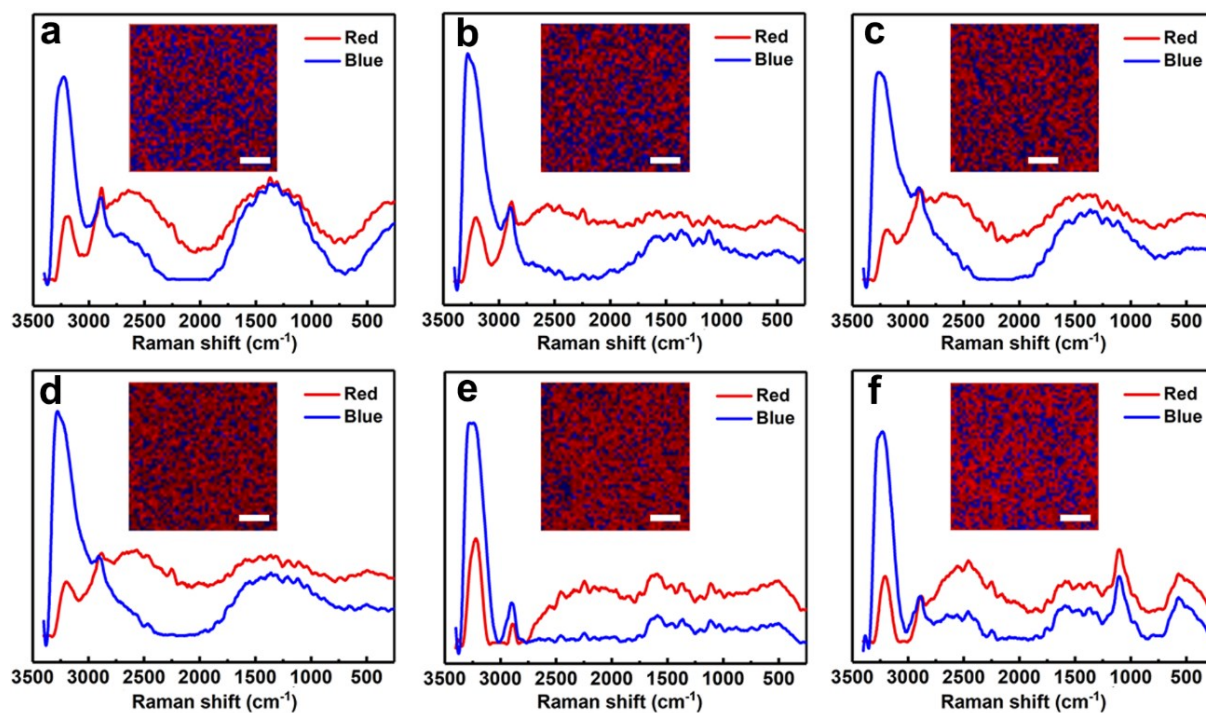


Fig. S6 Raman spectra of hydrophilic domains (blue) and hydrophobic domains (red) of a) CHTA0-60, b) CHTA2-60, c) CHTA4-60, d) CHTA6-60, e) CHTA10-60 and f) CHTA12-60 hydrogels. The insets are the reconstructed MCR Raman mappings of hydrophilic domains (blue) and hydrophobic domains (red) obtained from -OH and -NH stretching mode intensities ($3000\text{-}3400\text{ cm}^{-1}$). All bars are $50\text{ }\mu\text{m}$.

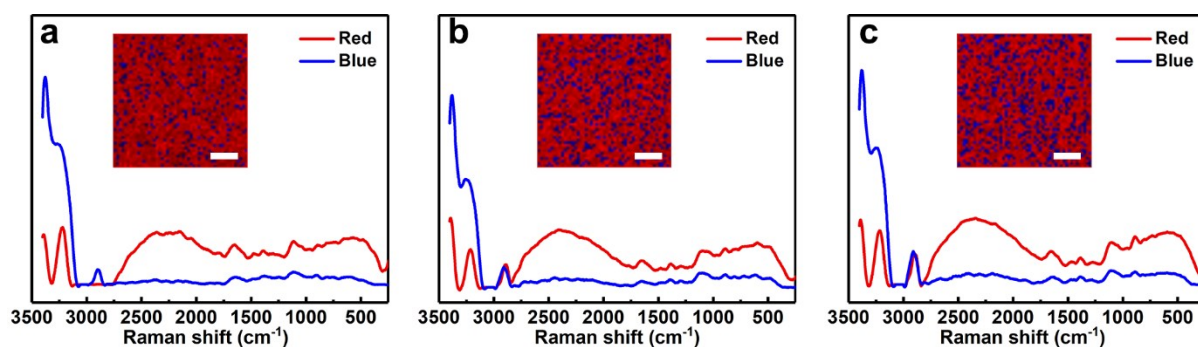


Fig. S7 Raman spectra of hydrophilic domains (blue) and hydrophobic domains (red) of **a)** CHTA8-0, **b)** CHTA8-20 and **c)** CHTA8-40 hydrogels. The insets are the reconstructed MCR Raman mappings of hydrophilic domains (blue) and hydrophobic domains (red) obtained from -OH and -NH stretching mode intensities ($3000\text{-}3400\text{ cm}^{-1}$). All bars are $50\text{ }\mu\text{m}$.

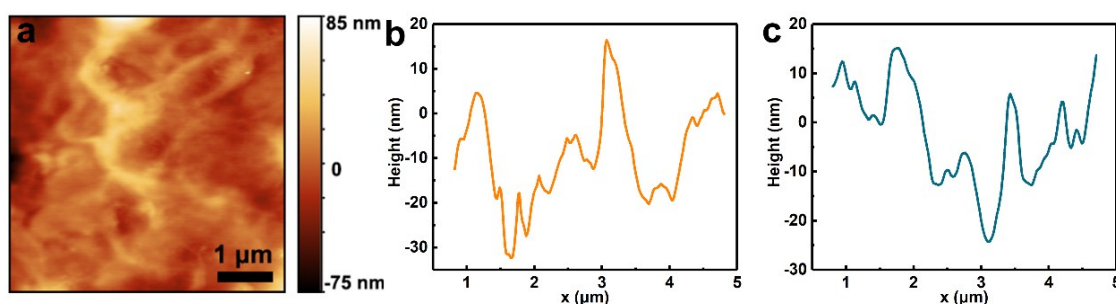


Fig. S8 **a)** AFM image and **b)** corresponding height histogram of CHTA0-60 hydrogel. **c)** Corresponding height histogram of CHTA8-60 hydrogel.

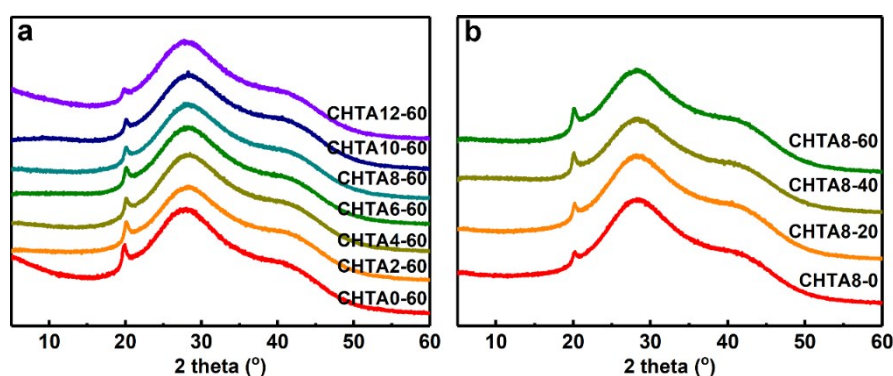


Fig. S9 XRD profiles from 5° to 60° of the CHTA0-60 and CHTA hydrogels with **a)** different weight ratios of tannic acid to chitin and **b)** aqueous ethanol concentrations.

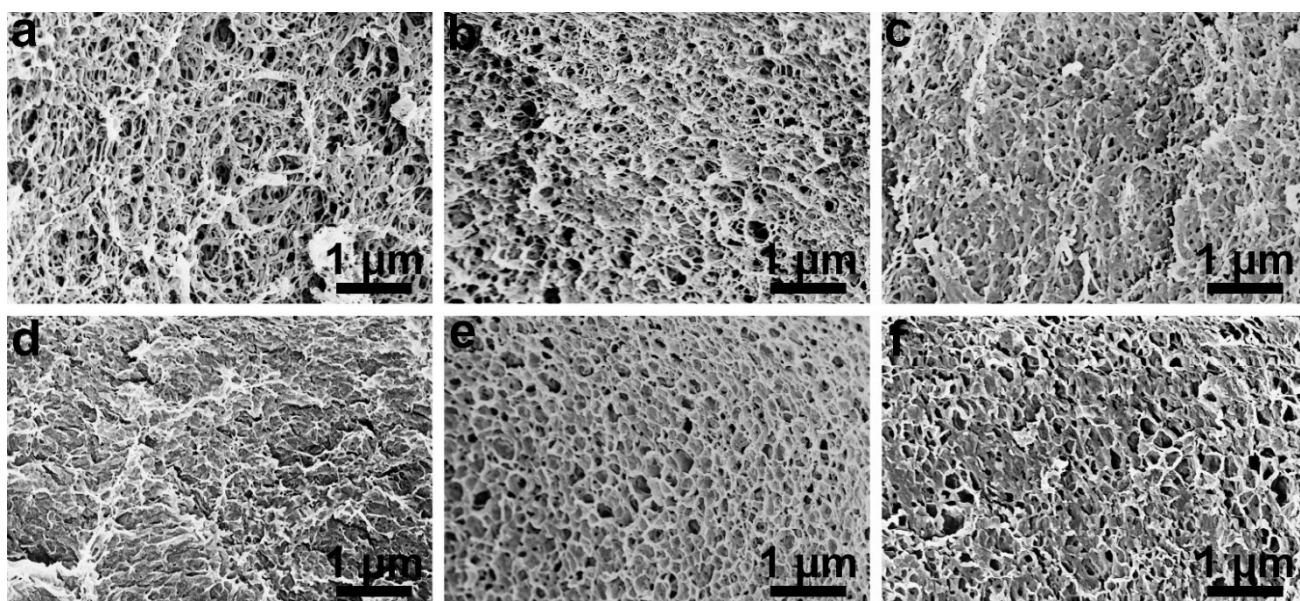


Fig. S10 SEM images of a) CHTA0-60, b) CHTA2-60, c) CHTA4-60, d) CHTA6-60, e) CHTA10-60 and f) CHTA12-60 lyophilized hydrogels.

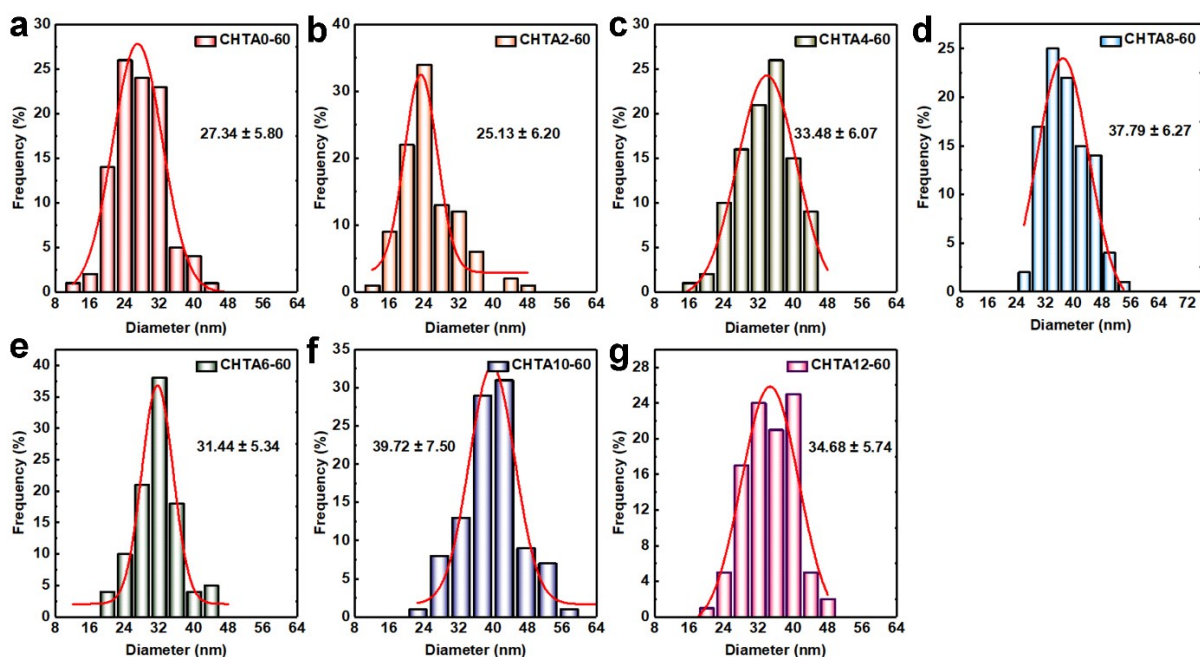


Fig. S11 Diameter distribution (calculated from SEM images) of a) CHTA0-60, b) CHTA2-60, c) CHTA4-60, d) CHTA6-60, e) CHTA8-60 f) CHTA10-60 and g) CHTA12-60 lyophilized hydrogels.

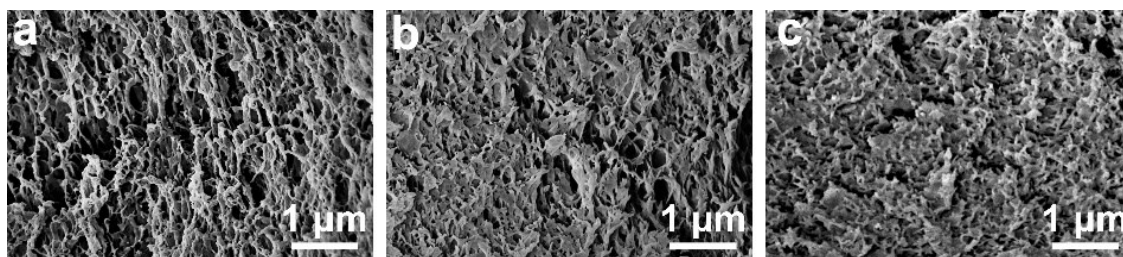


Fig. S12 SEM images of **a)** CHTA8-0, **b)** CHTA8-20 and **c)** CHTA8-40 lyophilized hydrogels.

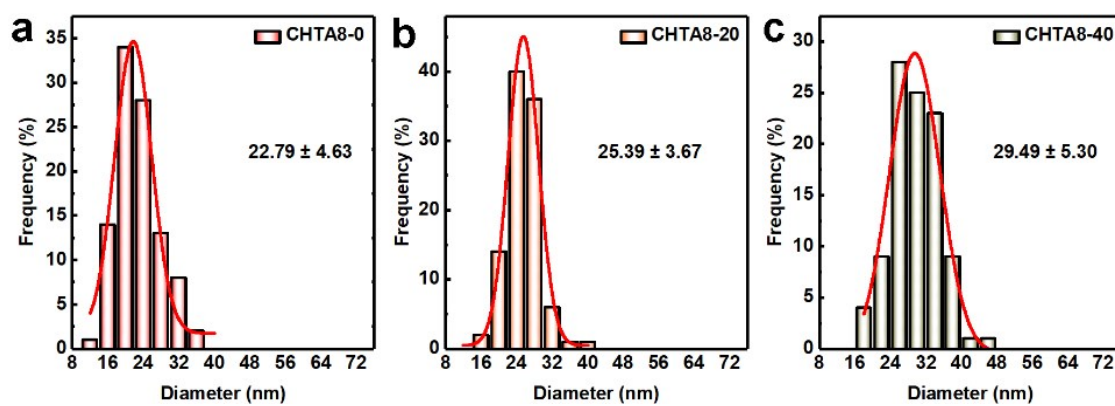


Fig. S13 Diameter distribution (calculated from SEM images) of **a)** CHTA8-0, **b)** CHTA8-20 and **c)** CHTA8-40 lyophilized hydrogels.

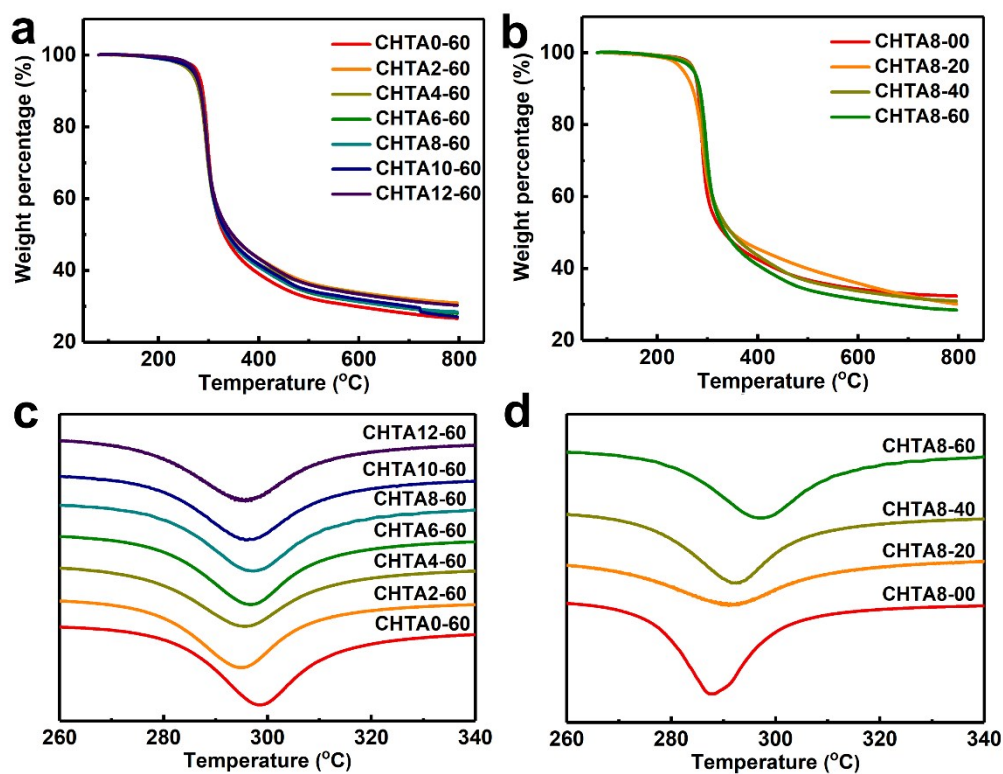


Fig. S14 TG curves of CHTA lyophilized hydrogels with **a)** different weight ratios of tannic acid to chitin and **b)** aqueous ethanol concentrations. DTG curves of CHTA8 lyophilized hydrogels with **c)** different weight ratios of tannic acid to chitin and **d)** aqueous ethanol concentrations.

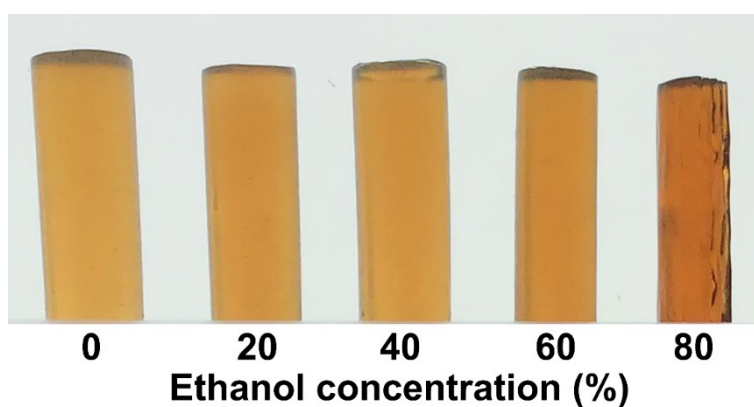


Fig. S15 Photos of CHTA8 hydrogels coagulating with different concentration ethanol solution.

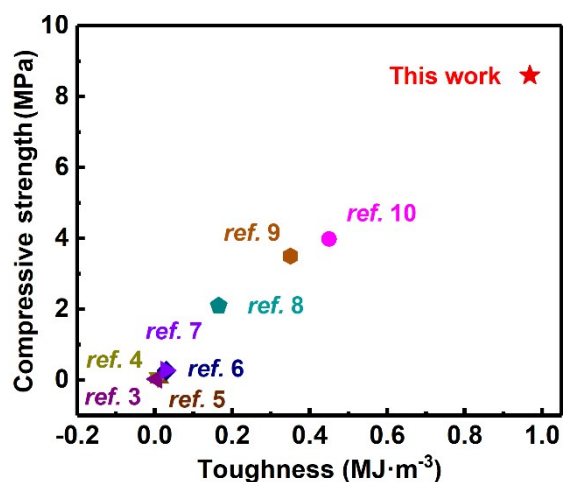


Fig. S16 A comparison of CHTA hydrogels, double-network chitin hydrogels, chemically-physically crosslinked chitin hydrogels and nanocomposite hybrid chitin hydrogels. *ref. 3*: chitin/halloysite composite hydrogel³, *ref. 4*: epichlorohydrin (ECH) crosslinked chitin/clay composite hydrogel⁴, *ref. 5*: ECH crosslinked chitin/tannic acid/graphene oxide composite hydrogel⁵, *ref. 6*: carboxymethyl chitin/tyramine hydrogel⁶, *ref. 7*: ECH crosslinked chitin/hydroxyapatite composite hydrogel⁷, *ref. 8*: ECH crosslinked chitin/PVA DN hydrogel⁸, *ref. 9*: TEMPO-chitin /polyacrylamide double-network hydrogel⁹ and *ref. 10*: ECH chemically-physically crosslinked chitin hydrogel¹⁰.

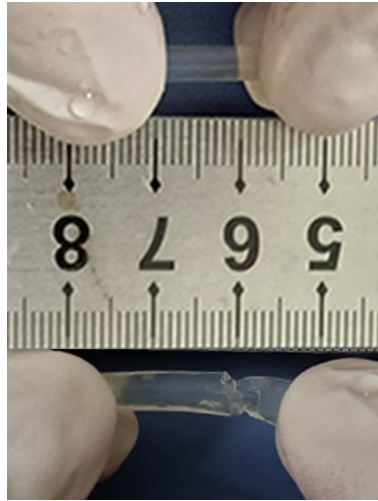


Fig. S17 Tensile behaviours of CHTA0-60 hydrogels.

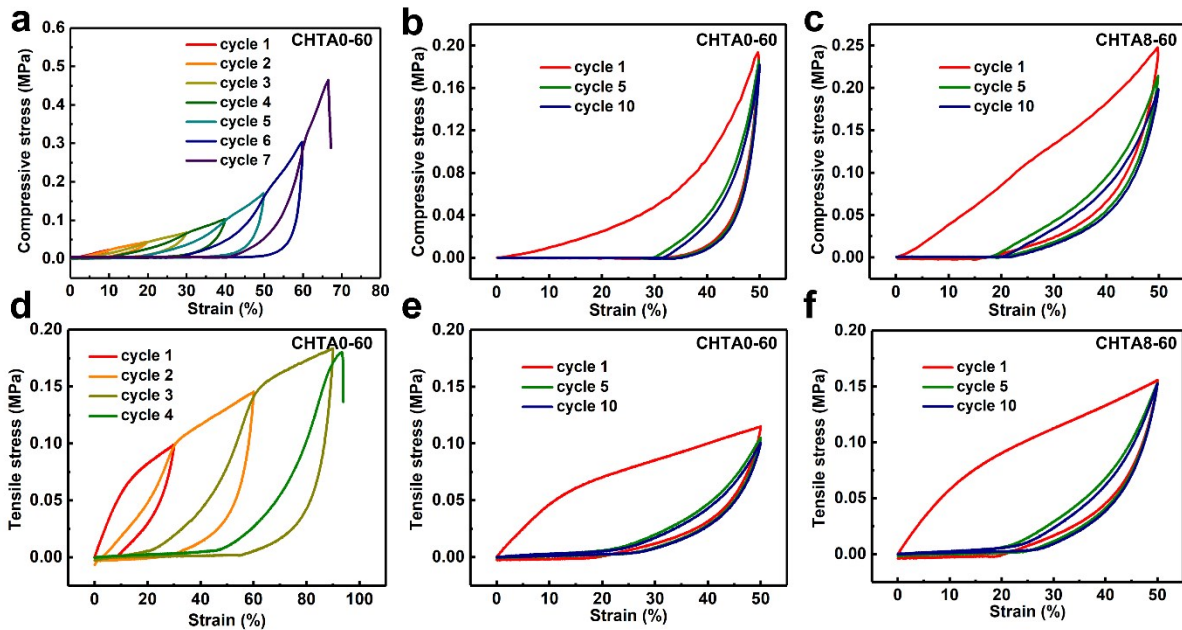


Fig. S18 **a)** The loading-unloading cycles with varying maximum compressions of CHTA0-60 hydrogels. The loading-unloading cycles of **b)** CHTA0-60 and **c)** CHTA8-60 hydrogels obtained from 10 repeated cycles up to a compression strain of 50%. **d)** The loading-unloading cycles with various maximum stretching of CHTA0-60 hydrogels. The loading-unloading cycles of **e)** CHTA0-60 and **f)** CHTA8-60 hydrogels obtained from 10 repeated cycles up to a tensile strain of 50%.

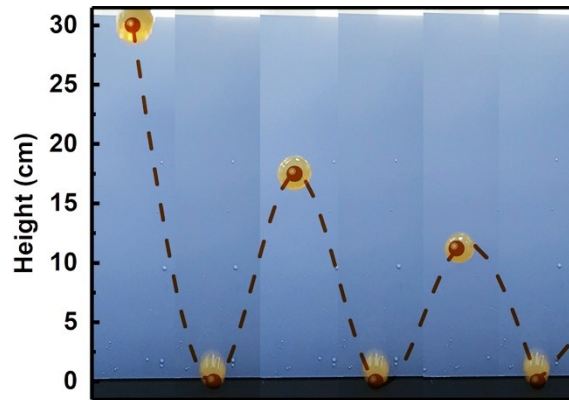


Fig. S19 Elasticity behaviours of CHTA8-60 hydrogels.

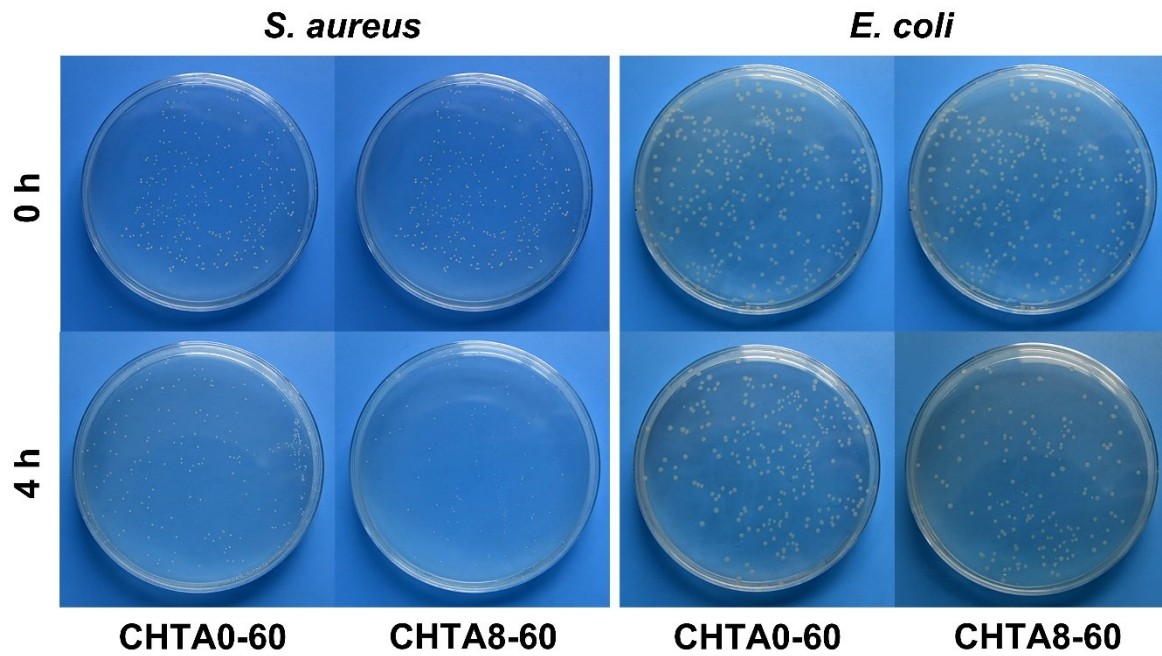


Fig. S20 Photos of antibacterial behaviours of CHTA0-60 and CHTA8-60 hydrogels after 4 h incubation at 37°C.

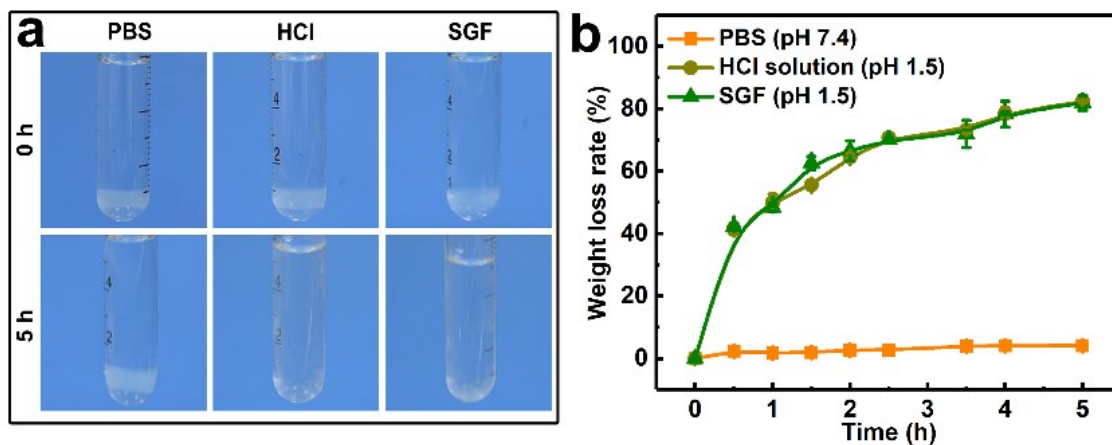


Fig. S21 a) Degradation photos and b) degradation curves of CHTA0-60 hydrogels in different solution after 5 h.

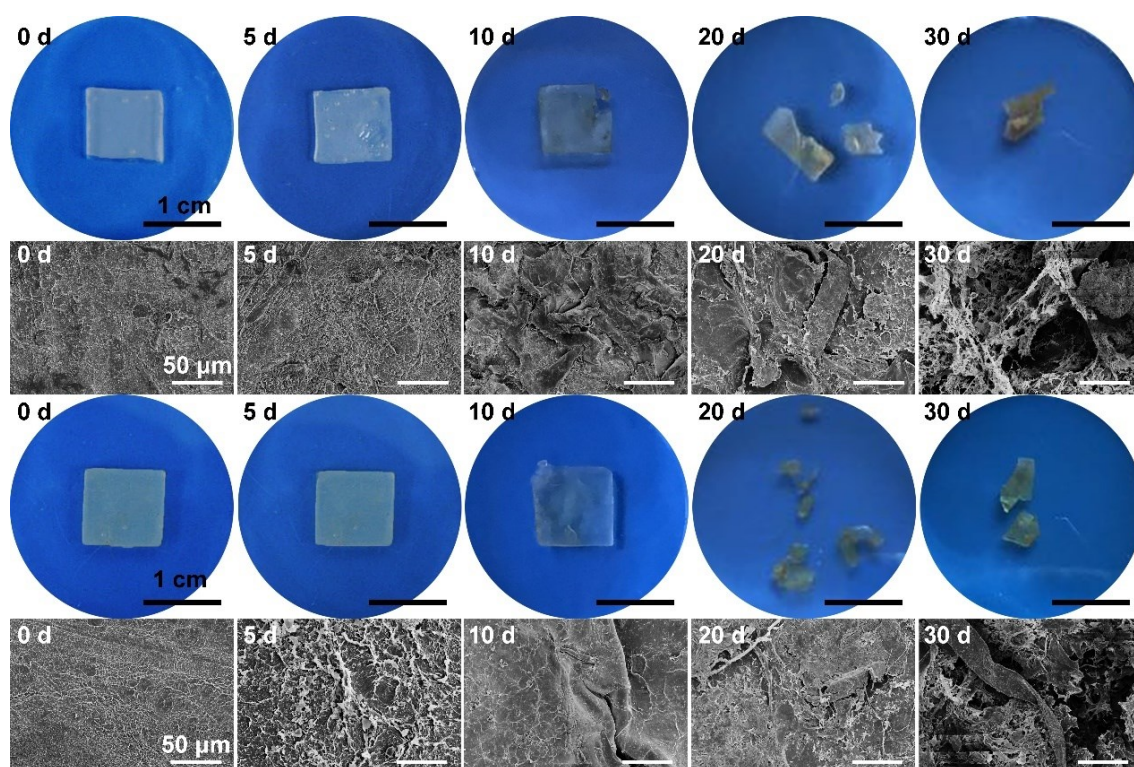


Fig. S22 Photos and corresponding images of CHTA0-60 (up) and CHTA8-60 (down) hydrogels degraded in soil for 0-30 days.

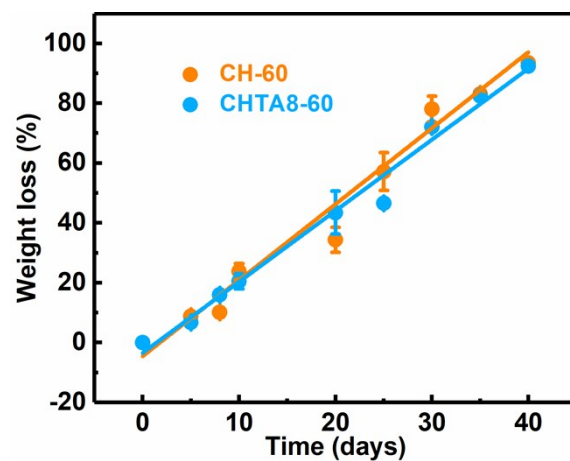


Fig. S23 Degradation curves of CHTA0-60 and CHTA8-60 hydrogels in soil.



Fig. S24 Degradation behaviours of CHTA8-60 hydrogel ball in soil for 100 days.

Supplementary references

- S1. Y. Huang, Y. Fang, L. Chen, A. Lu and L. Zhang, *Chem. Eng. J.*, 2017, **315**, 573-582.
- S2. A. P. Ault, D. I. Stark, J. L. Axson, J. N. Keeney, A. D. Maynard, I. L. Bergin and M. A. Philbert, *Environ. Sci-Nano*, 2016, **3**, 1510-1520.
- S3. X. Zhao, Y. Luo, P. Tan, M. Liu and C. Zhou, *Int. J. Biol. Macromol.*, 2019, **132**, 406-415.
- S4. M. Liu, Y. Zhang, J. Li and C. Zhou, *Int. J. Biol. Macromol.*, 2013, **58**, 23-30.
- S5. C. Liu, H. Liu, K. Tang, K. Zhang, Z. Zou and X. Gao, *J. Polym. Environ.*, 2020, **28**, 984-994.
- S6. B. Bi, H. Liu, W. Kang, R. Zhuo and X. Jiang, *Colloids. Surf. B*, 2019, **175**, 614-624.
- S7. C. Chang, N. Peng, M. He, Y. Teramoto, Y. Nishio and L. Zhang, *Carbohydr. Polym.*, 2013, **91**, 7-13.
- S8. M. He, Z. Wang, Y. Cao, Y. Zhao, B. Duan, Y. Chen, M. Xu and L. Zhang, *Biomacromolecules*, 2014, **15**, 3358-3365.
- S9. Y. Yue, X. Wang, Q. Wu, J. Han and J. Jiang, *J. Colloid. Interface. Sci.*, 2020, **564**, 99-112.
- S10. D. Xu, J. Huang, D. Zhao, B. Ding, L. Zhang and J. Cai, *Adv. Mater.*, 2016, **28**, 5844-5849.